Journal of Solid State Chemistry **145,** 511–516 (1999)
Article ID jssc.1999.8196, available online at http://www.idealibrary.com on IDEAL®

A Structural Study of the Quasi One-Dimensional Compound $(Ca_{1-x}Y_x)_{0.82}CuO_2$ Prepared at Room Pressure

Yuzuru Miyazaki,[1] Ian Gameson, and Peter P. Edwards[2]

School of Chemistry, University of Birmingham, Edgbaston, Birmingham B15 2TT, United Kingdom

Received September 21, 1998; in revised form February 2, 1999; accepted February 5, 1999

DEDICATED TO PROFESSOR PETER DAY FRS

A solid solution of the quasi one-dimensional cuprate, $(Ca_{1-x}Y_x)_{0.82}CuO_2$ ($0 \le x \le 0.435$), has been successfully synthesized in an oxygen stream at room pressure. Structural changes have been determined for the basic crystal structure by means of the Rietveld method using powder X-ray diffraction. Upon Y doping, the nearest (intrachain) Cu–Cu distance increases from 1.93 to 1.98 Å, while the next-nearest (interchain) Cu–Cu distance decreases from 3.46 to 3.41 Å. The incommensurate superstructure, originating from differences in the periodic arrangement of the (Ca, Y) atoms and CuO_2 chains, has also been examined. The modulation period along the crystal *a* axis implies that the stoichiometry of the solid solution shifts toward that of the cation-deficient member $(Ca_{1-x}Y_x)_{0.80}CuO_2$. This compositional discrepancy might be canceled by the large change in the modulation period along the *c* axis. © 1999 Academic Press

INTRODUCTION

Low-dimensional cuprates have recently attracted much interest since the discovery of superconductivity in the spin–ladder compound, $(Sr, Ca)_{14}Cu_{24}O_{41}$ (1). The crystal structure of the compound consists of two distinctive Cu–O networks (2). One is a Cu_2O_3 ladder comprised of two, edge-shared zig-zag chains. The other structural plaquette is an edge-shared square-planar CuO_2 chain, as seen in the $NaCuO_2$-type structure (3). These ladders and chains stack alternatively along the *b* axis to form a low-dimensional structure. It is inevitable that the existence of both ladders and chains in $(Sr, Ca)_{14}Cu_{24}O_{41}$ complicates any detailed interpretation of its electronic structure. If either the ladders or the chains could be studied separately, a greater understanding of their respective behavior would be possible. Actually, there exist compounds which have either Cu_2O_3 ladders or CuO_2 chains in the Sr–Cu–O system, namely $SrCu_2O_3$ (4) and $Sr_{0.73}CuO_2$ (5), respectively. However, both compounds can only be synthesized under high pressures. The compound $Ca_{1-y}CuO_2$ ($y \sim 0.15$) (6, 7), on the other hand, which has the one-dimensional edge-shared CuO_2 chains, can be synthesized at room pressure. In Fig. 1 we show the crystal structure of $Ca_{1-y}CuO_2$ (7); the structure is essentially identical to those of $Sr_{0.73}CuO_2$ and $Ba_{0.67}CuO_2$ (8). Since these alkaline-earth cuprates usually have an in-built deficiency (5–8), an incommensurate superstructure arises from the periodic differences in the arrangements of alkaline-earth cations and the CuO_2 chains. As a result, the oxidation state of Cu ions exceeds two, even without changes in the oxygen stoichiometry. For example, the formal Cu valence of $Ca_{1-y}CuO_2$ is around $+2.3$, which implies that excess holes are introduced into the CuO_2 chains. Davies and co-workers (9, 10) reported that Y ions can substitute into about one half of the Ca sites to form a solid solution; the formula is usually represented as $Ca_{2+x}Y_{2-x}Cu_5O_{10}$ ($0 \le x \le 0.8$) instead of the formulation $(Ca_{1-x}Y_x)_{1-y}CuO_2$. The formal valence of Cu in the solid solution is reported to vary from $+2.00$ to $+2.16$, while all the samples show insulating behavior. It is important to interrogate the magnetic behavior of such a one-dimensional CuO_2 network in which the formal Cu valence changes continuously, without a fundamental change in the crystal structure. Dolinšek *et al.* (11) reported the magnetic susceptibility of $Ca_{0.85}CuO_2$ which showed a broad maximum at around 50 K, behavior typical of $S = 1/2$ Heisenberg chains (12). These authors claimed that the broad peak is attributable not to a spin-dimer but rather to even-number spin-fragments within the chains. Hayashi *et al.* (13) succeeded in preparing a wide range of Y-substituted samples using 215 bar of oxygen pressure and they reported their temperature dependence of the magnetic susceptibility. Miyazaki *et al.* (14) independently examined the solid solution, but now synthesized at room pressure, and measured

[1] Permanent address: Department of Applied Physics, Graduate School of Engineering, Tohoku University, Aramaki-Aoba, Aoba-ku, Sendai 980-8579, Japan.

[2] To whom correspondence should be addressed. E-mail: p.p.edwards@bham.ac.uk.

0022-4596/99 $30.00

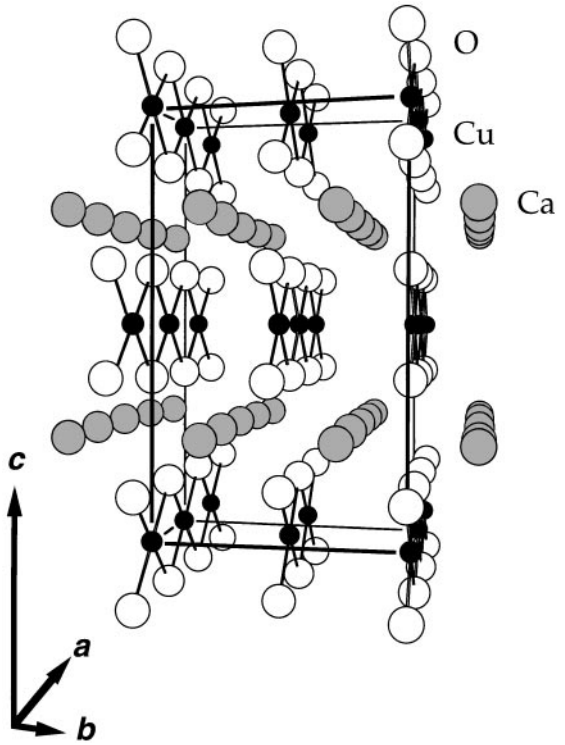

FIG. 1. The "ideal" basic crystal structure of $Ca_{1-y}CuO_2$.

the magnetic behavior. Although the preparation conditions and the composition of the samples are different between Hayashi *et al.* and Miyazaki *et al.*, the observed magnetic behavior was almost identical if the results were suitably scaled against the hole concentration in the CuO_2 chain. Both sets of samples showed a distinctive evolution in magnetic behavior from a dimer-like state to a long-range antiferromagnetically ordered state. The hole concentration thus appears to play a key role in determining the electronic structure of the title system. However, a complete structural study is required to characterize the solid solution system. Although some electron microscope studies have been carried out (9, 10, 15, 16), a detailed structural study for the entire solid solution range has not yet been reported. By applying a method reported by Davies (10) to our powder X-ray diffraction data, we have successfully determined the superlattice periods for the title compounds. Here we report a detailed structural study of the solid solution $(Ca_{1-x}Y_x)_{0.82}CuO_2$ ($0 \le x \le 0.435$), including a determination of the incommensurate superstructure.

EXPERIMENTAL

Polycrystalline samples were prepared from high-purity $CaCO_3$ (99.9%), Y_2O_3 (99.99%), and CuO (99.99%) powders. Intimate mixtures of these fine-sieved powders were heated at a temperature between 830 and 1000°C for appropriate periods with intermediate grindings. All the samples were fired in flowing oxygen at room pressure. The optimum sintering conditions were found to be closely dependent on the sample composition; the samples with $0 \le x < 0.15$, $0.15 \le x \le 0.30$, and $0.30 < x \le 0.45$ were synthesized at 830°C for total heating times of 360 h, at 880°C for 192 h, and 980°C for 144 h, respectively.

X-ray powder diffraction (XRD) data were collected at room temperature in the angular range 10°–100° with a 2θ step of 0.020° using a Siemens D5000 diffractometer. The basic structure was determined by the X-ray Rietveld analysis using the Rietan-97 program (17) excluding the peaks of superstructure. Interatomic distances and angles were then computed using a program "ORFFE" (18).

RESULTS AND DISCUSSION

Basic Structure

The basic structure was determined using a structural model first proposed by Babu and Greaves (7). The refined structural parameters and final R values are presented in Table 1 with the structure model. In the refinement procedure, the isotropic thermal parameter of the O atom was fixed at 1.0. All the positional parameters converged to reasonable values. We observed that the splitting of the fundamental $\{111\}$ and $\{113\}$ peaks, at around $2\theta = 36°$ and 43°, became significant with increasing Y content x. This peak splitting might be attributed to a structural change to a lower symmetry. The large R values obtained for the samples with higher x values almost certainly originate from this poor profile-fitting for these $\{111\}$ and $\{113\}$ peaks. Further electron microscopic study is necessary to investigate the symmetry of the samples with higher x values. As reported for the $Ca_{0.85}CuO_2$ phase (7), large thermal parameters of the (Ca, Y) atoms and Cu atoms imply that both atoms deviate from the ideal sites in the actual modulated structure.

In Fig. 2 we show the effect of Y substitution on the crystal lattice parameters of the basic unit cell. The magnitude of estimated standard deviations (esd's) of all the values are within the data points shown. For comparison, the results obtained under different preparation conditions, in air by Davies (10), and under 215 bar of oxygen by Hayashi *et al.* (13), are also shown. The data from these sources were fitted so as to represent the relative Y content, x in $(Ca_{1-x}Y_x)_{0.82}CuO_2$. The crystal a axis length, which reflects the nearest Cu–Cu distance along the CuO_2 chain, gradually increases with increasing x and appears to saturate at higher x values. The substitution of smaller trivalent Y ions (0.90 Å, $CN = 6$) (19) for divalent Ca ions (1.00 Å) has a significant effect on the b axis length, while the c axis length remains almost constant. Similar effects have also been observed for samples prepared under high oxygen pressure (13). The differences in the absolute values of those lattice

TABLE 1
Summary of the Final *R* Factors and the Refined Structural Parameters for $(Ca_{1-x}Y_x)_{0.82}CuO_2$ ($0 \le x \le 0.435$)

x	R_{WP} (%)	R_P (%)	R_e (%)	R_I (%)	a (Å)	b (Å)	c (Å)	$x_{(Ca,Y)}$	$B_{(Ca,Y)}$ (Å^2)	B_{Cu} (Å^2)	y_O	z_O
0	6.28	4.00	3.69	5.30	2.8056(1)	6.3208(1)	10.5765(2)	0.390(1)	1.36(11)	1.39(5)	0.048(1)	0.6222(3)
0.05	7.98	5.20	4.33	3.95	2.8092(1)	6.3093(2)	10.5763(3)	0.390(1)	1.45(11)	1.84(5)	0.050(1)	0.6230(3)
0.10	9.42	6.11	4.89	4.23	2.8125(1)	6.2968(4)	10.5742(4)	0.391(1)	1.84(12)	1.85(5)	0.051(1)	0.6226(3)
0.15	9.14	5.68	4.78	4.35	2.8153(1)	6.2860(3)	10.5775(4)	0.393(2)	2.68(14)	2.37(7)	0.053(1)	0.6230(4)
0.20	10.23	6.46	4.50	4.81	2.8186(1)	6.2645(2)	10.5714(4)	0.391(1)	2.03(13)	1.56(6)	0.053(1)	0.6236(4)
0.25	10.60	6.59	4.29	5.17	2.8206(1)	6.2519(3)	10.5743(5)	0.392(2)	2.53(14)	1.55(6)	0.056(1)	0.6241(4)
0.30	12.30	7.78	4.50	5.35	2.8268(1)	6.2356(4)	10.5743(4)	0.388(1)	2.36(13)	1.47(6)	0.057(1)	0.6254(4)
0.35	15.74	10.40	4.04	6.99	2.8265(1)	6.2216(2)	10.5754(4)	0.383(1)	1.61(13)	0.65(7)	0.053(1)	0.6252(5)
0.40	14.47	9.40	4.53	5.83	2.8278(1)	6.2134(2)	10.5867(4)	0.383(1)	2.26(13)	1.28(7)	0.053(1)	0.6260(4)
0.435	15.21	9.48	4.73	7.51	2.8269(1)	6.2061(2)	10.5930(4)	0.383(2)	2.12(15)	1.02(8)	0.054(1)	0.6265(5)

Basic structure model (7): *Fmmm* (No. 69), $Z = 4$.

Atom	Site	occ.	x	y	z	B_{iso}
(Ca, Y)	16*l*	0.205	$x_{(Ca,Y)}$	1/4	1/4	$B_{(Ca,Y)}$
Cu	4*a*	1.0	0	0	0	B_{Cu}
O	16*m*	1/2	0	y_O	z_O	1.0

parameters can be rationalized in terms of the differences in both synthesis pressure and composition. Compared to the samples prepared by Hayashi *et al.* (13), our samples have slightly higher concentration of Ca and Y atoms; the formula of their samples can be represented as $(Ca_{1-x}Y_x)_{0.80}CuO_2$. The cell volume calculated from these lattice parameters decreased monotonically from 187.6(1) Å^3 ($x = 0$) to 185.8(1) Å^3 ($x = 0.435$); these were consistently about 0.5% larger than those reported by Hayashi *et al.*

Next, we determined the effect of Y substitution on the coordination of Cu and O atoms. In Figs. 3a and 3b we show the x dependence on the Cu–O distance in the CuO_2 chain and on the nearest Cu–Cu distance between the CuO_2 chains along the b axis, respectively. Upon Y doping (increasing x), the Cu–O distance in the CuO_2 chains gradually increases from 1.932(2) to 1.976(4) Å. These values are typical of those seen in the compounds having four-coordinated CuO_2 square-planar polyhedra (20, 21). As previously reported, the oxygen content remains at 2.00, within experimental error, throughout the entire Y substitution range studied here (14). This increase in the Cu–O distance can be rationalized by a decrease in the hole carrier concentration. In contrast to the nearest (intrachain) Cu–O distance, the next-nearest (interchain) Cu–Cu distance linearly decreases from 3.458(1) to 3.410(1) Å. These values are about 0.2 Å shorter than the Cu–Cu distance in the similar one-dimensional compound, Li_2CuO_2 (21). As shown in Fig. 2, the nearest Cu–Cu distances (related to the a axis length) along the chain are 2.81–2.83 Å ($=a$), which is slightly shorter than that found in Li_2CuO_2 (2.86 Å). Since both the intra- and interchain Cu–Cu distances in the present system are smaller than those in Li_2CuO_2, a substantial direct interaction between the Cu^{2+} spins is anticipated. Actually, the samples with higher x ($Cu^{n+} \sim 2.0$) show a Néel temperature (T_N) of ~ 29 K, which is much higher than that of Li_2CuO_2, $T_N = 8.3$ K. With decreasing x, long-range magnetic order gradually collapses due to both the increase in the next-nearest (interchain) Cu–Cu distances, and the introduction of spins; the latter may form magnetically inactive ($S = 0$) spin singlets. Therefore, the system with lower Y contents ($Cu^{n+} > 2.2$) tends to exhibit a one-dimensional nature in the magnetic behavior (13, 14).

In Fig. 4 we show the O–Cu–O angles in the CuO_2 chain, α, plotted against the compositional parameter x. The basic structure model utilizing the *Fmmm* space group results in a planar coordination of the Cu and O atoms in the CuO_2 chain, where $\beta = 180^\circ - \alpha$. Since the Y substitution causes a gradual decrease in the α angle (with a concomitant increase in the β angle), one might expect that the CuO_2 chain shrinks along the longitudinal direction. However, a large increase in the Cu–O distance (Fig. 3a) due to electron-doping expands the CuO_2 chain (equivalent to the a axis length) toward its longitudinal direction.

Superstructure

The solid solution has an incommensurate superstructure along the a and c axes, due to the periodic differences in the arrangement of (Ca, Y) atoms and the CuO_2 chains. In Fig. 5 we show the powder (2θ range 29°–45°) of the solid

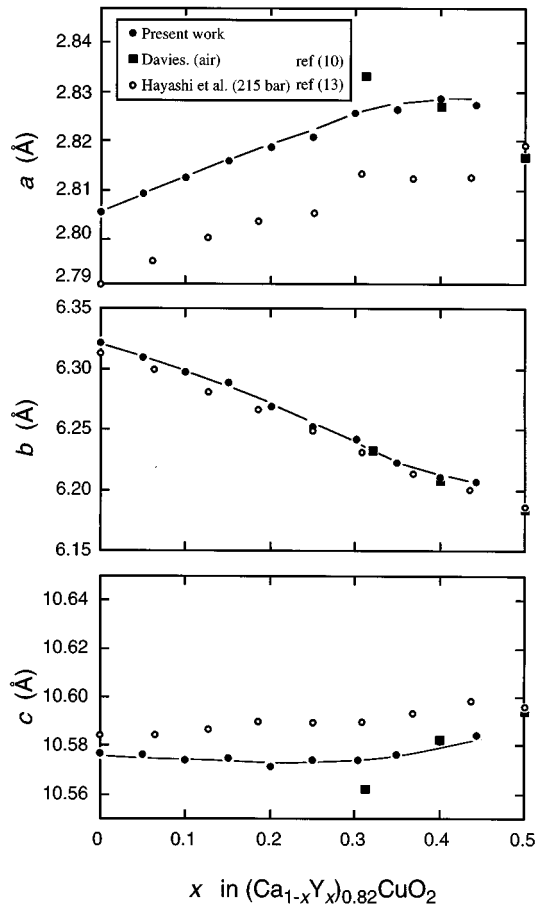

FIG. 2. Effect of Y substitution on the lattice parameters of the basic unit cell.

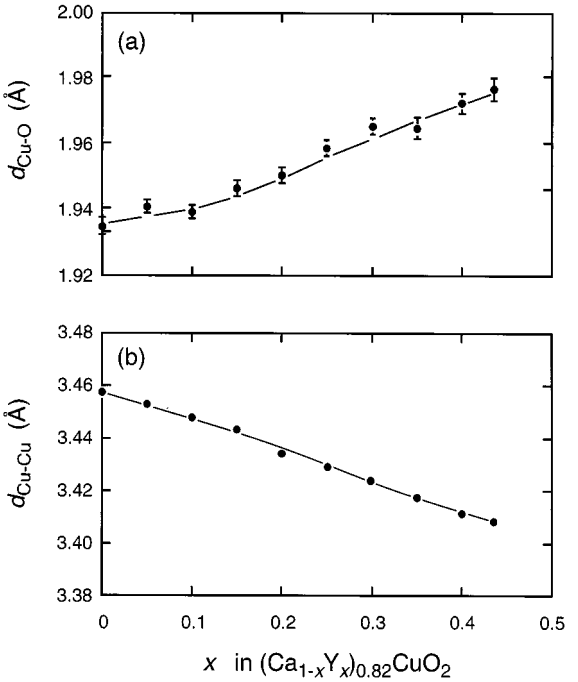

FIG. 3. Effect of Y substitution on the Cu–O length in the CuO_2 chain (a), and on the nearest Cu–Cu length between the CuO_2 chains (b).

solution. Besides the fundamental {022}, {004}, {111}, and {113} reflections, four intense peaks originating from the incommensurate superstructure can be clearly seen. Two peaks with lower 2θ values are the $\{1-\delta_a, 1, 1-\delta_c\}$, and $\{1-\delta_a, 1, 1+\delta_c\}$ statellite peaks of the fundamental {111} peak and the other two peaks are $\{1-\delta_a, 1, 3-\delta_c\}$ and $\{1-\delta_a, 1, 3+\delta_c\}$ satellites of the {113} peaks. A rather weak diffraction peak (labeled "*" in Fig. 5) just below the fundamental {022} reflection in 2θ does not originate from impurities, but to the $\{-\delta_a, 2, 2-\delta_c\}$ peaks of the superstructure. The incommensurate periods along the a and c axes, a_{sup} and c_{sup}, are defined as $a_{sup} = a/\delta_a$ and $c_{sup} = c/\delta_c$, respectively (10). Then, we performed curve-fitting for those superstructure peaks using a pseudo-Voigt function. The resulting d values were converted to δ_a and δ_c values using the crystallographic equation $1/d_{hkl}^2 = h^2/a^2 + k^2/b^2 + l^2/c^2$ for an orthorhombic cell. In Fig. 6 we show the derived incommensurate superlattice periods plotted against x. The value a_{sup} is almost constant at lower x; then gradually changes from $6.02(3)a$ to $5.16(3)a$, to give a stoichiometry of the samples from $Ca_{0.834}CuO_2[Ca_{1-1/6.02}CuO_2]$ to $(Ca,Y)_{0.806}CuO_2[(Ca,Y)_{1-1/5.16}CuO_2]$, even when samples were prepared with the $(Ca,Y)_{0.82}CuO_2$ composition. This compositional discrepancy might be compensated by a stacking fault, as frequently observed in the solid solution prepared in air (10, 16), and a large periodic change in the modulation along the c axis. Actually, the incommensurate period along the c axis c_{sup}, significantly changes from $6.29(3)c$ to $3.97(3)c$ with increasing x. The data

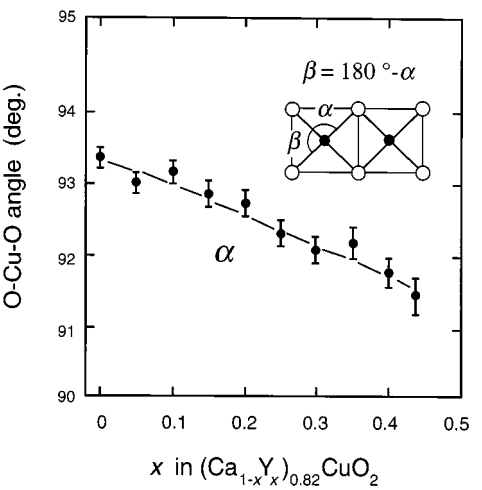

FIG. 4. Effect of Y substitution on the O–Cu–O angles in the CuO_2 chain.

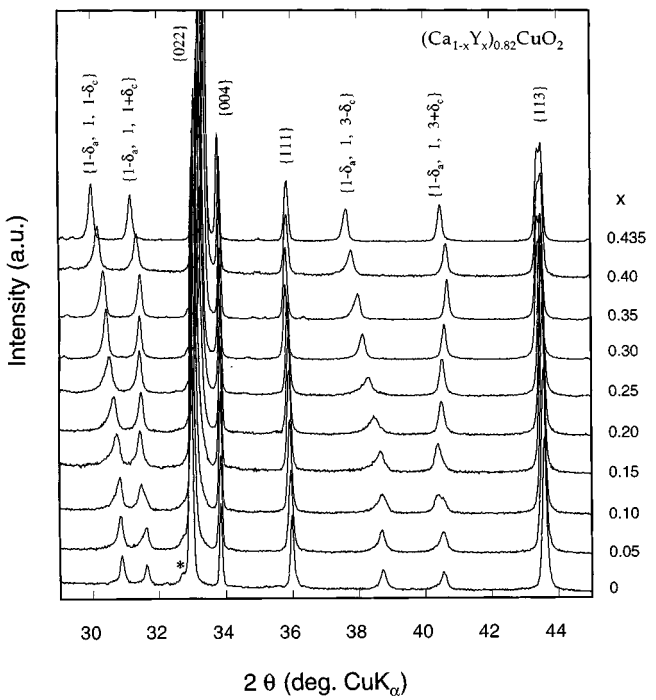

FIG. 5. XRD patterns of the $(Ca_{1-x}Y_x)_{0.82}CuO_2$ solid solution. Four intense superlattice peaks shift significantly upon Y doping.

reported by Davies (10) are recalculated for our compositional formula $(Ca_{1-x}Y_x)_{0.80}CuO_2$ and are also shown in Fig. 6. The data of Davies can be accurately superimposed (after conversion to our composition formulation) on our curves even though the nominal compositions and the lattice parameters are different. It should be noted that the single-phase region tends to slightly shift toward the (Ca, Y)-poor composition upon Y doping under 1 atm of O_2 (14). Furthermore, the stoichiometry of the pure-Ca phase is reported to be ca. $Ca_{0.83}CuO_2$ (using our formula) by several authors (6, 7, 15, 16), while the Y-rich phases are often represented as $(Ca, Y)_{0.80}CuO_2$ (9, 10, 13). Therefore, the derived data for the δ_a value may represent the universal composition curve in this solid solution system. All the data shown so far exhibit a gradual change with changes in the compositional parameter x, whereas δ_c shows a large change above $x = 0.15$. As reported elsewhere (14), the solid solution shows a long-range magnetic order below 29 K for the sample with $x > 0.20$ (a result shown in the inset of Fig. 6). If the figure is turned upside-down, one may reflect on a possible relationship between T_N and δ_c against x. We have no direct evidence to connect these phenomena at present.

The displacement of the (Ca, Y) atoms from the ideal position of the basic structure can be adequately described by a simple sine wave along the a axis, although the amplitude was not determined. In Figs. 7a and 7b we show a representation of the basic structure and the proposed corresponding superstructure projected along the b axis. The thick rectangle in Fig. 7a represents the basic unit cell; a displacement of the atoms is emphasized in Fig. 7b. Consider as an example the supercell of an end-member of the solid solution, $(Ca_{0.565}Y_{0.435})_{0.82}CuO_2$. The compound has supercell parameters ($a_{sup} = a/\delta_a$ and $c_{sup} = c/\delta_c$) of $a_{sup} = 5.16a$ and $c_{sup} = 3.97c$, as shown in Fig. 6. In this superstructure, each layer of the (Ca, Y) atoms has a sine-wave modulation along the c axis. The retardation between the adjacent (Ca, Y) layers is expressed by $\delta_c\pi$ and then $2\delta_c\pi$ for the adjacent unit cell. Thus, the phase matches every 3.97 (nearly 4) unit cells along the c axis ($c_{sup} = 3.97c$). The reason twinstructures are often observed (10, 16) can be explained by the fact that the modulation period along the

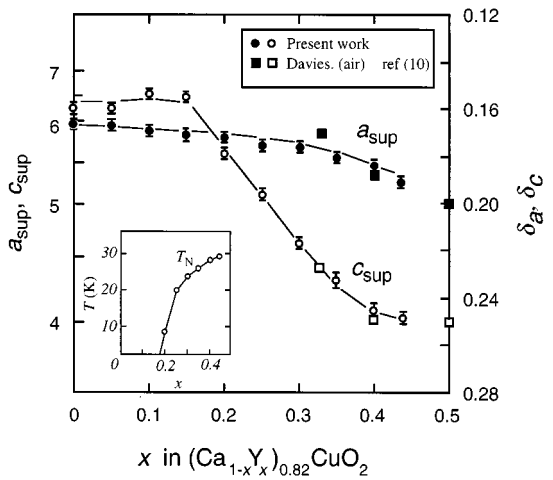

FIG. 6. Calculated incommensurate periods along the a and c axes, $a_{sup} = a/\delta_a$ and $c_{sup} = c/\delta_c$, plotted against the Y content, x. The plot for the Néel temperature, T_N, against x is shown in the inset.

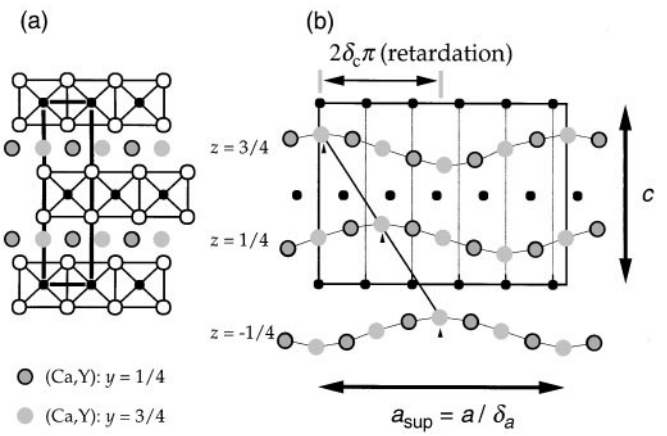

FIG. 7. Basic unit cell projected along the b axis (a) and schematic representation of the proposed incommensurate superstructure for the $(Ca_{1-x}Y_x)_{0.82}CuO_2$ solid solution.

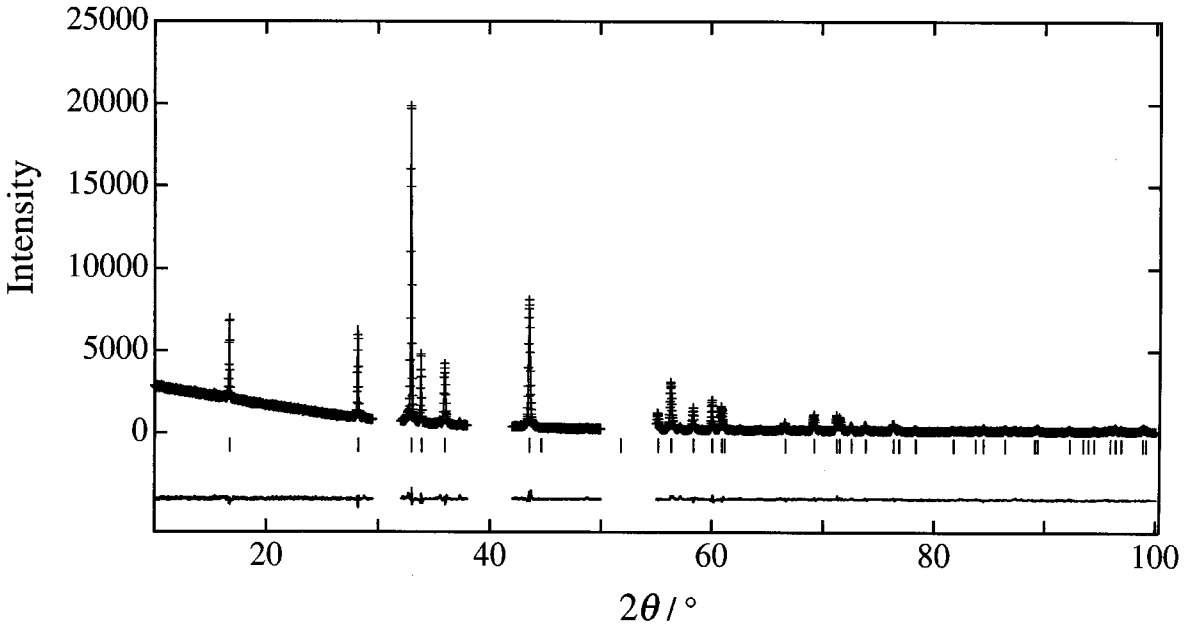

FIG. A. Observed (dotted) and calculated (solid line) XRD profile for $Ca_{0.82}CuO_2$.

c axis is not an integer for most solid solutions. As a result of the displacement of the (Ca, Y) atoms, the arrangement of the CuO_2 chains must clearly be affected. The relatively large thermal parameters of the Cu atom (B_{Cu}, Table 1) implies that the Cu atom also has a displacement for a certain direction. Babu and Greaves (7) reported that the Cu atom in $Ca_{0.85}CuO_2$ has a large anisotropic thermal displacement perpendicular to the CuO_2 chains. Similarly, small rotational buckling of the CuO_2 chains toward the *b* axis is probably realized in this solid solution. This displacement of the Cu atoms might cause some spin modulation in its magnetic structure. To clarify details of the magnetic structure, a powder neutron diffraction study is currently underway.

APPENDIX

In Fig. A we show the result of the Rietveld refinement for $Ca_{0.82}CuO_2$ as an example. Four peaks at approx. 2θ values of 31°–32° and 38°–41° originating from the superstructure are excluded in the refinement.

ACKNOWLEDGMENT

We thank the JSPS (Japan Society for the Promotion of Science) for the award of a Postdoctoral Fellowships for Research Abroad to Y.M.

REFERENCES

1. M. Uehara, T. Nagata, J. Akimitsu, H. Takahashi, N Mori, and K. Kinoshita, *J. Phys. Soc. Jpn.* **65,** 2764 (1996).
2. E. M. McCarron, III, M. A. Subramanian, J. C. Calabrese, and R. L. Harlow, *Mater. Res. Bull.* **23,** 1355 (1988).
3. N. E. Brese, M. O'Keeffe, R. B. von Dreele, and V. G. Young, *J. Solid State Chem.* **83,** 1 (1989).
4. Z. Hiroi, M. Azuma, M. Takano, and Y. Bando, *J. Solid State Chem.* **95,** 230 (1991).
5. J. Karpinski, H. Schwer, G. I. Meijer, K. Conder, E. M. Kopnin, and C. Rossel, *Physica C* **274,** 99 (1997).
6. T. Siegrist, R. S. Roth, C. J. Rawn, and J. J. Ritter, *Chem. Mater.* **2,** 192 (1990).
7. T. G. N. Babu and C. Greaves, *Mater. Res. Bull.* **26,** 499 (1991).
8. J. G. Thompson, J. D. Fitz Gerald, R. L. Withers, P. J. Barlow, and J. S. Anderson, *Mater. Res. Bull.* **24,** 505 (1989).
9. P. K. Davies, E. Caignol, and T. King, *J. Am. Ceram. Soc.* **74,** 569 (1991).
10. P. K. Davies, *J. Solid State Chem.* **95,** 365 (1991).
11. J. Dolinšek, D. Arčon, P. Cevc, O. Milat, M. Miljak, and I. Aviani, *Phys. Rev. B* **57,** 7798 (1998).
12. J. C. Bonner and M. E. Fisher, *Phys. Rev. A* **135,** 640 (1964).
13. A. Hayashi, B. Batlogg, and R. J. Cava, *Phys. Rev. B* **58,** 2678 (1998).
14. Y. Miyazaki, N. C. Hyatt, I. Gameson, M. Slaski, and P. P. Edwards, submitted for publication.
15. O. Milat, G. van Tendeloo, S. Amelinckx, T. G. N. Babu, and C. Greaves, *Solid State Commun.* **79,** 1059 (1991).
16. O. Milat, G. van Tendeloo, S. Amelinckx, T. G. N. Babu, and C. Greaves, *J. Solid State Chem.* **97,** 405 (1992).
17. F. Izumi (1993), *in* "The Rietveld Method" (R. A. Young Ed.), Chap. 13.
18. W. R. Busing, K. O. Martin, and H. A. Levy, Report ORNL-TM-306; Oak Ridge National Laboratory, TN, 1964.
19. R. D. Shannon, *Acta Crystallogr. A* **32,** 751 (1976).
20. M. A. Beno, L. Soderholm, D. W. Capone, II, D. G. Hinks, J. D. Jorgensen, J. D. Grace, I. K. Schuller, C. U. Serge, and K. Zhang, *Appl. Phys. Lett.* **51,** 57 (1987).
21. F. Sapiña, J. R. Carvajal, M. J. Sanchis, R. Ibáñez, A. Beltrán, and D. Beltrán, *Solid State Commun.* **74,** 779 (1990).